Journal of Colloid and Interface Science 604 (2021) 248–259

Contents lists available at ScienceDirect

Journal of Colloid and Interface Science

journal homepage: www.elsevier.com/locate/jcis

Interfacial kinetics in olive oil-in-water nanoemulsions: Relationships between rates of initiation of lipid peroxidation, induction times and effective interfacial antioxidant concentrations

Marlene Costa [a], Josefa Freiría-Gándara [b], Sonia Losada-Barreiro [a,b], Fátima Paiva-Martins [a], Carolina Aliaga [c], Carlos Bravo-Díaz [b,*]

[a] Requimte-Laqv, University of Porto, Science Faculty, Dept. of Chemistry and Biochemistry, 4169-007 Porto, Portugal
[b] University of Vigo, Chemistry Faculty, Dept. of Physical-Chemistry, 36310 Vigo, Spain
[c] Facultad de Química y Biología, Universidad de Santiago de Chile, Centro para el Desarrollo de la Nanociencia y la Nanotecnología, Cedenna, Av. B.O'Higgins 3363, Santiago, Chile

GRAPHICAL ABSTRACT

Olive oil nanoemulsions are treated as a three-compartment system consisting of a lipid, aqueous and interfacial compartments with different solvent properties. The oxidation of a lipid, the partitioning of an antioxidant and the chemical reaction between them are indicated.

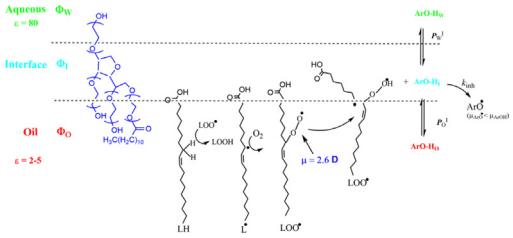

ARTICLE INFO

Article history:
Received 15 February 2021
Revised 11 June 2021
Accepted 17 June 2021
Available online 1 July 2021

Keywords:
Lipid peroxidation
Induction periods
Rate of initiation
Antioxidant concentration
Emulsions

ABSTRACT

Hypothesis: A detailed quantitative description of the effects of antioxidants in inhibiting lipid peroxidation in oil-in-water emulsions can be achieved by determining the relationships between the rates of initiation of the lipid peroxidation reaction, the length of the induction period preceding the propagation step of the radical oxidation process and the effective antioxidant interfacial concentrations.
Experiments: We successfully prepared and characterized a series of olive oil-in-water nanoemulsions and allowed them to spontaneously oxidize. Their oxidative stability was evaluated by carrying out in the presence, and absence, of antioxidants derived from gallic acid, by monitoring the formation of primary oxidation products with time, by determining the corresponding induction periods, and by determining the effective interfacial concentrations of the antioxidants in the intact emulsions.
Findings: Results show that both, the length of the induction periods and the antioxidant interfacial concentrations change concomitantly, increasing with the hydrophobicity of the antioxidant up to a maximum at the octyl derivative; longer aliphatic chains decrease their efficiency. The ratio between the interfacial antioxidant concentration and the induction period remains constant independently of the antioxidant, demonstrating that the effective concentrations of antioxidant at the interface control their efficiencies in emulsions.

* Corresponding author.
E-mail address: cbravo@uvigo.es (C. Bravo-Díaz).

https://doi.org/10.1016/j.jcis.2021.06.101
0021-9797/

1. Introduction

Lipids are a major source of energy in foods and are necessary for supplying essential fatty acids to humans [1,2]. In addition, lipids play a crucial role in determining the physico-chemical properties of foods including their flavor, texture and appearance [3–5]. Nevertheless, their ingestion is not free of risks because they may oxidize spontaneously when in contact with air, producing harmful products, and because over-consumption may increase dangerously the concentration of cholesterol and saturated fats in blood and in other parts of the organism. The oxidation of polyunsaturated fatty acids, PUFAs, is the main chemical reaction involved in the deterioration of alimentary oils and fats, and its currently believed that it may participate in the damage to cell structures caused by reactive oxygen species and in toxic processes that lead to cell collapse [1,6,7].

The lipid oxidation reaction is commonly described in terms of the formation, propagation and termination of lipid radicals, generating a variety of breakdown harmful products such as including aldehydes, ethers, ketones and alcohols [8–10]. A simplified version of the mechanism is shown in Scheme 1, where only the relevant steps (reactions (1)–(4)) are displayed.

The lipid oxidation reaction can be effectively controlled by addition of antioxidants, reactions (5)–(6) in Scheme 1 [11–13]. The kinetic profiles of the inhibited peroxidation processes, Scheme 2, are usually characterized by a slow buildup of primary oxidation products (conjugated dienes, CDs) in time followed by a faster production of CDs (propagation reaction). In the presence of antioxidants, the lipidic radicals produced in the system (reaction (3)) react with the antioxidant (reaction (5)) minimizing the production of by-products through the reactions (3) and (4). During this relatively slow step (inhibition reaction (5)), the rate of peroxidation is time-dependent, and the reaction continues until the almost total consumption of the antioxidant. When the antioxidant concentration is nearly depleted, the inhibition reaction becomes un-inhibited, and the rate of the overall oxidation reaction increases [10,14–16].

On the basis of Scheme 1, one can define as "efficient antioxidants" those molecules whose rate of trapping radicals, r_{inh}, is equal to, or higher than, the rate of radical production r_p [17–19]. Graphically, the relative efficiency of antioxidants can be assessed on the basis of the kinetic profiles by comparing the lengths of the induction periods τ_{ind} in the absence (control experiment) and in the presence of the antioxidants, Scheme 2; the longer the τ_{ind}, the higher the antioxidant efficiency [20,21].

Efficient antioxidants include tocopherols, catechols, cinnamates, catechins, and gallates, that are widely employed in the food, pharmaceutical, and cosmetic industries to minimize or inhibit lipid oxidation [10,22]. Because of their potential health benefits, big efforts are continuously made in the search of new efficient antioxidants derived from hopeful natural sources. Big efforts are also made in developing new strategies to incorporate them to prepare stable high added-value formulations against oxidation and degradation of parenteral emulsions, lipid-based cosmetics or foodstuffs [23,24].

Loading nanoemulsions with new antioxidants with tailored characteristics to achieve optimal antioxidant efficiency and/or nutritional effects is tricky and not always possible. For example, the selection of antioxidants to be employed in particular foods or in nutritional (parenteral) nanoemulsions depends on the regulatory status of AOs [25]. A potentially practical and useful alternative approach is to chemically modify potent natural antioxidants to retain their reactive moiety but to optimize their hydrophilic-lipophilic balance (HLB), an example of it is to attach inert alkyl chains of different length to the reactive antioxidant moiety. For instance, propyl and lauryl gallates are food-approved antioxidants (E numbers 310 and 312, respectively) because, in addition to their intrinsic nutritional/health/redox properties, introduction of the alkyl chains of different length increases their hydrophobicity compared to that of the parent (hydrophilic) gallic acid [26,27]. The main consequence of these chemical changes is the modification of the distribution of the antioxidants in the various regions of emulsions or cellular membrane systems in accordance with their relative solubility in each region [17,18,28–31].

This strategy embodies the main objective of the present study in which we have successfully formulated and characterized olive oil-in-water nanoemulsions and used them as carriers of a number of gallic acid alkyl derivatives to optimize their antioxidative properties. The prepared nanoemulsions are oxidized in different extents, and our results show a direct relationship between the length of the lag phases (induction periods) and the interfacial concentrations of the antioxidants. This important finding comes out from the results of two totally independent set of experiments, and can be considered key factor to understand the kinetics of the lipid peroxidation reactions that takes place at the interfaces of multiphasic systems [20,32]. A second important outcome of

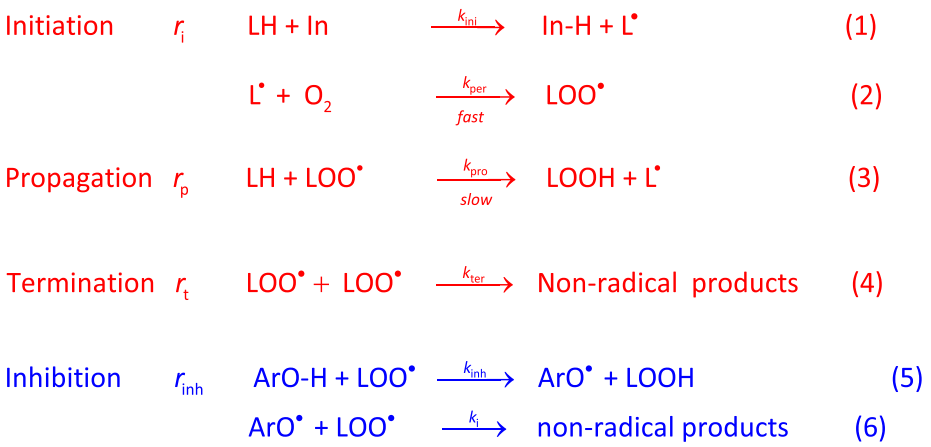

Scheme 1. Mechanism for the lipid oxidation reaction comprising the initiation (i), propagation (p) and termination (t) steps. For the sake of simplicity, only the slow (rate-determining) step of the propagation sequence is shown. The oxidation reaction may be hampered by addition of effective antioxidants (ArO-H) that regenerate the parent lipid by donation of an H-atom to the peroxyl radical. This set of reactions is valid assuming that [O_2] is large enough to convert all C-centered radicals (L$^\bullet$) into alkylperoxyl ones (LOO$^\bullet$). Further details on the mechanism of the reactions can be found elsewhere. In: any initiator, LH: unsaturated fatty acid, ArOH: antioxidant, LOO$^\bullet$: peroxyl radical, ArO$^\bullet$: radical derived from the antioxidant.

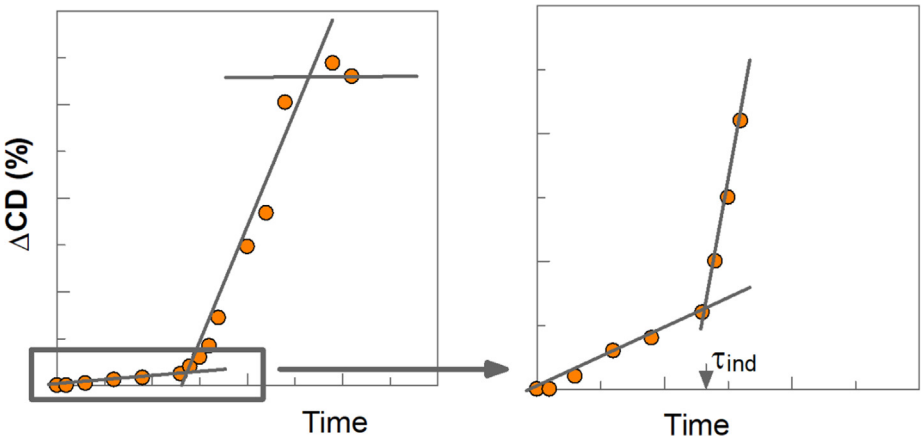

Scheme 2. Classic kinetic profile for a lipid oxidation reaction in the presence of an inhibitor (e.g., antioxidant) showing the (slow) formation of peroxidation products (conjugated dienes) as monitored spectrophotometrically at 234 nm. The chart on the right is an amplification of the lower part of the kinetic profile and shows the initial stage of peroxidation and some of the characteristic kinetic points. Once the antioxidant is consumed, uninhibited peroxidation of unsaturated fatty acids occurs more rapidly up to a maximum, after which the rate decreases due to the reduced concentration of substrate. The solid lines in the scheme were added on purpose to aid the eye and to illustrate the determination of τ_{ind}.

the work is the finding of unassailable experimental evidence that the interfacial region is the main site where the reaction between the AOs and lipid radicals take place, showing the need of determining quantitatively the effective concentrations of the antioxidants in the interfacial region, in order to correctly tackling the kinetics of lipid peroxidation, as much as the determination of lipid oxidation rates. On the other hand, the proposed methods enable quantization of antioxidant "efficiencies" in models relevant to biological systems by employing reliable, trustable, assays. They also illustrate a practical way to investigate the optimization of the antioxidative interfaces of oil-in-water nanoemulsions relevant to parenteral nutrition, cosmetics and other pharmaceutical formulations [33–35].

2. Experimental

2.1. Materials and methods

2.1.1. Materials

Extra virgin olive oil was obtained from a local supplier and was stripped from their endogenous antioxidants, to avoid interferences with the added antioxidants. Removal of endogenous polyphenols and tocopherols was done following literature procedures [36,37]. The absence of tocopherols was confirmed by HPLC (IUPAC method 5.4.32). To minimize the oxidation of the stripped oil, it was kept in the dark at low temperature. The chemical structures of the main fatty acids of olive oil are shown in Scheme 3.

Gallic acid and alkyl gallates, Scheme 3, were purchased from Across Organics and used without further purification. The non-ionic tensioactive Tween 80 (Scheme 3, Fluka) was of the maximum purity available (>99%) and employed as received. Aqueous buffered solutions were prepared with citric acid and sodium citrate (Across organics, pH = 3.6, [Buffer] = 0.04 M) to minimize potential oxidation by trace metals present in the oil.

All aqueous solutions were prepared with deionized water (resistivity > 18 MΩ cm).

2.2. Preparation of olive oil-in-water nanoemulsions

Initial coarse 1:9 (o/w, vol:vol) emulsions were prepared homogenizing at room temperature (T = 20–22 °C) mixtures of the stripped oil, the aqueous acid (buffered) solution and different amounts of surfactant volume fractions ($\Phi_I = V_{surf}/V_{emulsion}$) with the aid of a high-speed rotor (Polytron PT 1600 E, 20,000 rpm for 2 min).

Nanoemulsions were prepared by passing the coarse emulsion three times through an high pressure microfluidizer (Microfluidics, LM20 Microfluidizer) working at 25,000 Psi (137.5 MPa). To minimize a potential oxidation of the unsaturated lipids of the oils during the preparation process, the temperature of the nanoemulsions was decreased with the aid of an ice-bath.

Nanoemulsions were stored in the dark at T = 4 °C, but their physical characterization was carried out at room temperature. Droplet sizes and polydispersity indexes were calculated by dynamic light scattering (DLS) with the aid of a Malvern Mastersizer MS 3000 (Malvern Instruments Ltd., UK). ζ-potential values were determined by employing a particle electrophoresis instrument (Zetasizer Nanoseries Nano-ZS, Malvern Instruments, Worcestershire, UK). The physical stability of the nanoemulsions was determined for surfactant volume fractions Φ_I ($\Phi_I = V_{surf}/V_{emulsion}$) from 0.0047 to 0.045. In all cases, the physical stability of the nanoemulsions was higher than 3 months.

2.3. Oxidative stability of the nanoemulsions

The chemical stability of the nanoemulsions was determined in the absence and in the presence of antioxidants, by monitoring the formation of conjugated dienes, CDs, with time according to published procedures [17,19,36,37]. Nanoemulsions containing different amounts of surfactant and antioxidants were introduced in an orbital shaker (500 r.p.m) in the dark at constant temperature (T = 60 ± 1 °C) ensuring a constant oxygen supply from surrounding air. Aliquots of the nanoemulsions were removed at selected times, diluted to 10 mL with EtOH (VWR, >99.9%) and the absorbance at λ = 234 nm was measured. All oxidation experiments were performed in triplicate and reported results were averaged.

2.4. Determination of distribution and interfacial concentrations of antioxidants in intact nanoemulsions

Since it is physically impossible to separate the interfacial region of the nanoemulsions without disrupting the existing equilibria, common analytical methods typically employed to determine analyte concentrations in bulk and binary systems cannot be employed to determine distributions of reactants in the intact nanoemulsions. To overcome the problem, we used the previously

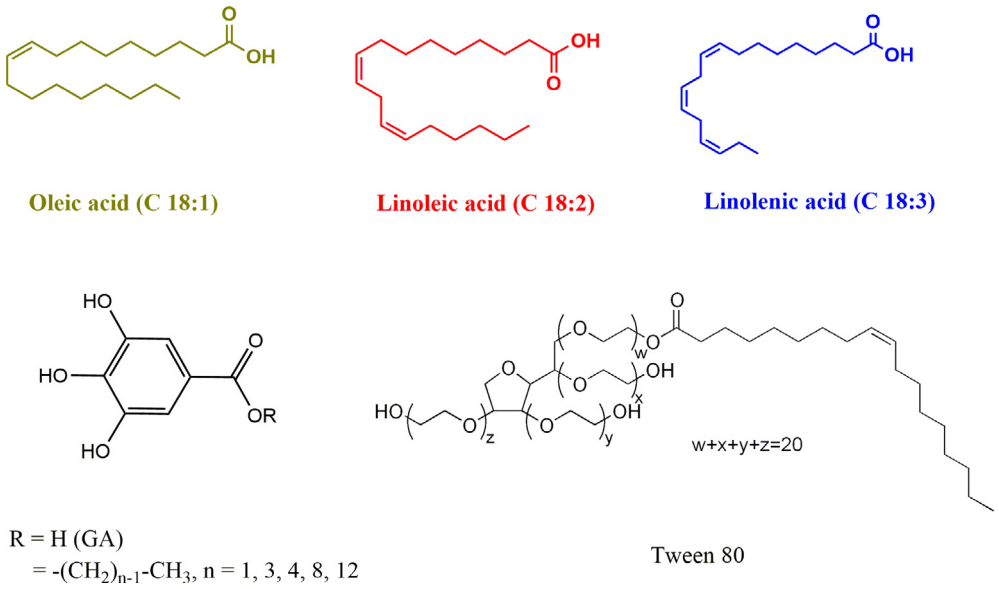

Scheme 3. Chemical structures of the main unsaturated fatty acids (*cis*-configuration) of olive oil, those of gallic acid (GA) and alkyl derivatives (C1, C3, C4, C8 and C12) employed in this work and of the surfactant Tween 80.

synthesized chemical probe 4-hexadecylbenzenediazonium (16-ArN_2^+) tetrafluoroborate, which reacts with virtually any antioxidant. For the sake of clarity, only a succinct description on the method is given here. Further details can be found elsewhere [29].

The method is based on the measurement of the observed rate constant, k_{obs}, for the reaction between the AOs and 16ArN_2^+ at different Φ_I values. The reactive group of 16ArN_2^+ is located in the interfacial region of the nanoemulsions, Scheme 4, where reacts with the antioxidants present in the region. The method for determining k_{obs} values in the intact nanoemulsions is available in detail elsewhere [29].

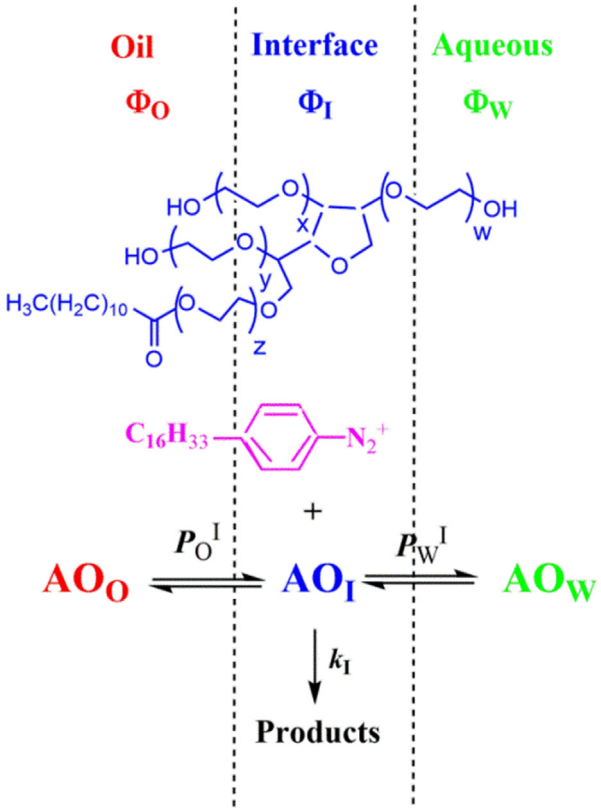

Scheme 4. Chart showing the dynamic allocation of an antioxidant AO in the aqueous, interfacial and oil regions of nanoemulsions and of the reactive $-N_2^+$ group of the chemical probe 16-ArN_2^+.

The rate constant values (k_{obs}) depend on both the medium properties and on the distribution of the antioxidant, and both contributions can be determined with the aid of the pseudophase kinetic model [29,38]. Simplifications can be made when considering oil-insoluble or water-insoluble antioxidants. Eqs. (1) and (2) define the partition constants of the antioxidants between the oil-interfacial and aqueous-interfacial regions, respectively (Scheme 4) and the kinetic Eqs. (3)–(5) describe the variations of k_{obs} with Φ_I. In Eqs. (1)–(5), concentrations given in brackets, $[AO_T]$, stand for the stoichiometric concentration (moles per liter of total volume of the nanoemulsion) meanwhile those given in parenthesis, (AO_O), (AO_I) and (AO_W), will stand for the effective concentrations in the oil, interfacial and aqueous regions, respectively, given in moles per liter of the particular region. This nomenclature for concentrations will be adopted hereafter.

Eq. (3) was employed for the water-insoluble AOs C8 and C12, Eq. (4) was used for oil-insoluble AOs GA and C1 and Eq. (5) for those AOs of intermediate hydrophobicity such as propyl gallate (C3). The linear plots of $1/k_{obs}$ *versus* Φ_I (not shown) were employed to determine P_O^I, P_W^I and k_I values. Calculations and procedures are detailed elsewhere [29]

$$P_O^I = \frac{(AO_I)}{(AO_O)} \quad (1)$$

$$P_W^I = \frac{(AO_I)}{(AO_W)} \quad (2)$$

$$k_{obs} = \frac{[AO_T]k_I P_O^I}{\Phi_I P_O^I + \Phi_O} \quad (3)$$

$$k_{obs} = \frac{[AO_T]k_I P_W^I}{\Phi_I P_W^I + \Phi_W} \quad (4)$$

$$k_{obs} = \frac{[AO_T]k_I P_W^I P_O^I}{\Phi_O P_W^I + \Phi_I P_W^I P_O^I + \Phi_W P_O^I} \quad (5)$$

Once the P^I_O and P^I_W values are known, the percentages of the antioxidants in the aqueous, (%AO_W), interfacial (%AO_I) and oil (%AO_O) regions can be determined by using Eqs. (6)–(8) [29]

$$\%AO_I = \frac{100\Phi_I P^I_O P^I_W}{\Phi_O P^I_W + \Phi_I P^I_O P^I_W + \Phi_W P^I_O} \quad (6)$$

$$\%AO_I = \frac{100\Phi_I P^I_W}{\Phi_I P^I_W + \Phi_W} \quad (7)$$

$$\%AO_I = \frac{100\Phi_I P^I_O}{\Phi_I P^I_O + \Phi_O} \quad (8)$$

Eqs. (6)–(8) are used to determine the fraction of AOs in the interfacial region (depending on the hydrophobicity of the AO), and analogous equations were employed to obtain the percentage of the AOs in the oil and aqueous regions. Details of the calculations are given elsewhere [29,36,39].

The effective concentrations in the oil, interfacial and aqueous regions are calculated by considering the number of moles n of the antioxidant and the volume of the particular region as shown in Eq. (9) for the interfacial region. Similar equations were employed to calculate (AO_W) and (AO_O) [29,38,40].

$$(AO_I) = \frac{n_I}{V_I} = \frac{[AO_T](\%AO_I)}{\Phi_I} \quad (9)$$

2.5. Statistical analyses

Oxidation experiments were carried out in triplicate. Reactions between 16-ArN^+_2 and the AOs were were run for at least 2–3 half-lives in duplicate or triplicate and the measured k_{obs} values were within ±6–8% with typical correlation coefficients > 0.995. Data were analyzed by one-way analysis of variance (ANOVA, with Tukey's test) with the level of significance set at P less than 0.05. Values are given as means ± standard deviation.

3. Results and discussion

3.1. Preparation, characterization and physical stability of stripped olive oil nanoemulsions.

In attempting to prepare nanoemulsions with the lowest droplet sizes as possible, we determined the minimum amount of cycles that were necessary to pass the coarse emulsions. The coarse olive emulsions were highly polydisperse, showing a bimodal distribution, inset in Fig. 1A, with average droplet sizes of d = (1248 ± 128) nm when employing a surfactant volume fraction $\Phi_I = V_{surf}/V_{emulsion}$ = 0.0047, and d = (478 ± 58) nm (Φ_I = 0.038). Constant droplet sizes values with monomodal droplet size distributions were found after three cycles Fig. 1A.

The variations of the average (mean) droplet size (MDS) and of the polidispersity index (PDI) with Φ_I are shown in Fig. 1B and 1C, respectively. As shown in Fig. 1B, the MDS of the nanoemulsions decreases upon increasing the surfactant concentration reaching a constant value when Φ_I > 0.015. PDI values are around 0.22 and are independent of surfactant concentration, indicating that the prepared nanoemulsions can be considered essentially monodisperse in contrast to the coarse emulsion (see inset in Fig. 1A).

To quantitatively asses the kinetic stability of the olive nanoemulsions, we computed the variations of the MDS of the prepared nanoemulsions with time, Fig. 2A. The mean droplet size remained constant for more than 16 days and no signs of phase separation or destabilization (coalescence, flocculation, creaming, etc.) were detected by naked eye for more than 60 days. The ς-potential values remained constant with time (results not shown) and with Φ_I, Fig. 2B. Low ς values, ranging from −12 to −17 mV, were otherwise expected since we employed Tween 80, a non-ionic surfactant, to stabilize kinetically the nanoemulsions. Results are qualitatively similar to those previously reported [23].

3.2. Effects of gallic acid and its alkyl derivatives on the kinetics of lipid oxidation: Oxidative stability of olive oil-in-water nanoemulsions

The kinetics of production of primary oxidation products (conjugated dienes, CDs) was obtained by examining the formation of CDs with time, Fig. 3A, in keeping with the AOCS Ti 1a-64 method. The induction period τ_{ind} values were obtained from the intersection of the two straight lines during and after the lag phase (Scheme 2). The variation of τ_{ind} with the number of C atoms in the alkyl chain of the AOs is shown in Fig. 3B. For the sake of comparisons, we also assessed the relative efficiency of the antioxidants by determining the time necessary to increase the formation of CDs in 0.5% (dashed line in Fig. 3A). As shown in Fig. 3B and C, both variations parallel each other, indicating that they are quantitatively similar and that both kinetic parameters can be employed indistinctively to assess the relative efficiency of the antioxidants.

The non-linear variation of τ_{ind} and t(ΔCD(0.5%)) with the hydrophobicity of the AOs has already been observed in emulsions loaded with different antioxidants and is generally known as the "cut-off effect", illustrating a non-linear dependence in a given property of homologous series of reactants with the number of C-atoms in their alkyl chains [29,36,41–43].

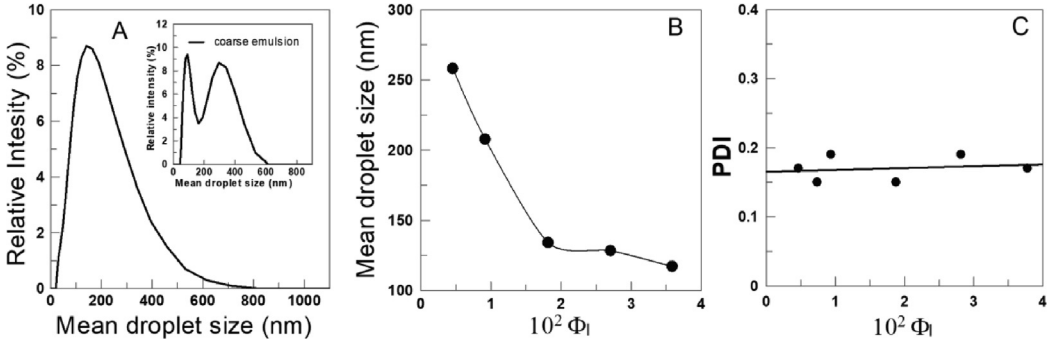

Fig. 1. (A) Dynamic light scattering, DLS, plots of coarse 1:9 olive O/W emulsions (inset) and nanoemulsions. (B, C) Changes of mean droplet size, MDS, (B) and of the polidispersity index PDI (C) with Φ_I.

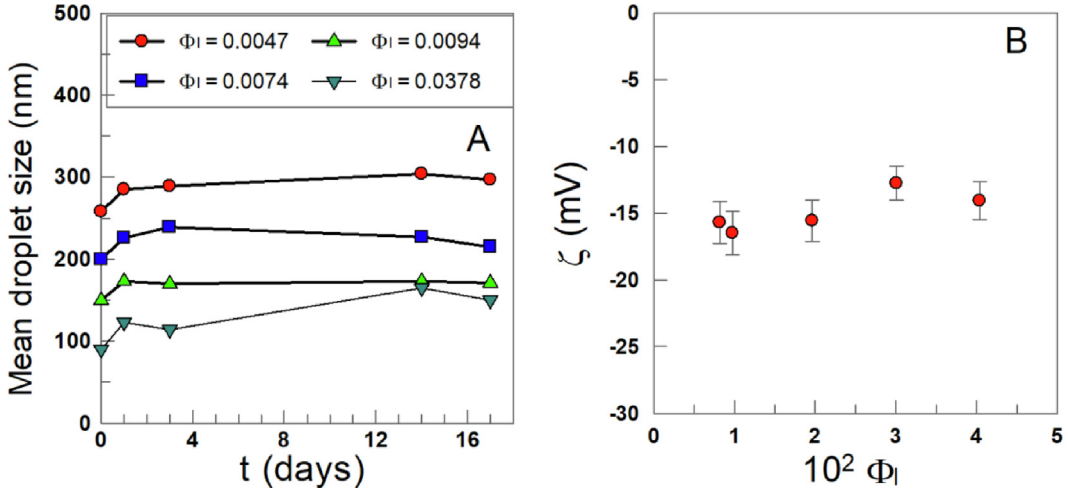

Fig. 2. (A) Variations of the mean droplet size with time of 1:9 (vol:vol) olive oil nanoemulsions prepared with different surfactant volume fractions Φ_l. (B) Changes in ς-potential of nanoemulsions droplets with Φ_l.

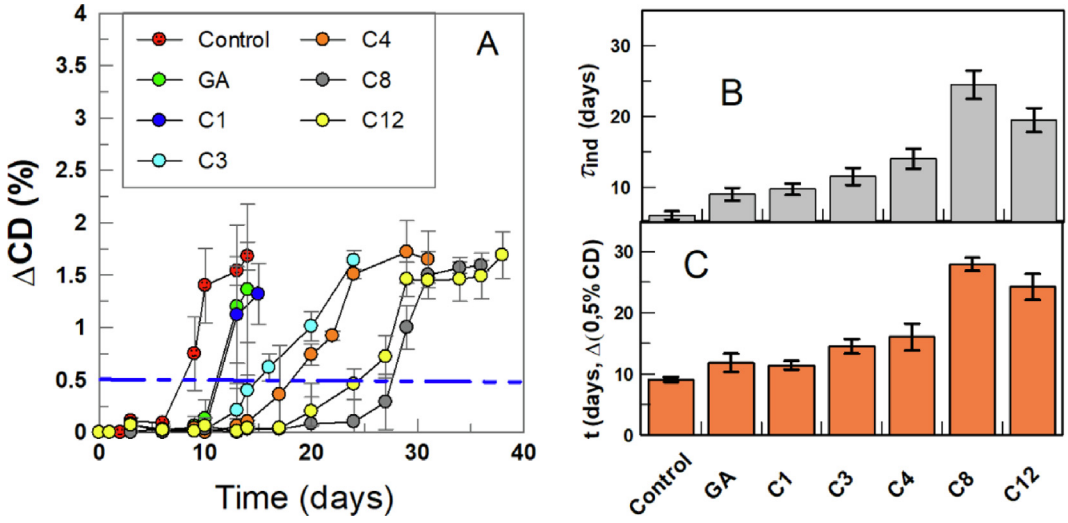

Fig. 3. (A) Variation in the formation of CDs (expressed as %) with time in 1:9 (vol:vol) stripped olive oil-in-water nanoemulsions (Φ_l = 0.0047) at T = 60 °C. The control sample contained no antioxidants because we used olive oil free of endogenous antioxidants. The variations of the induction period τ_{ind} and t(ΔCD(0.5%)) with the length of the alkyl chain is displayed in figure (B) and (C), respectively.

3.3. Distribution and interfacial concentrations of gallic acid derivatives in in olive oil nanoemulsions

The physical impossibility of separating the oil and aqueous regions from the interfacial one makes that any attempt to determine reliable values for the distribution of AOs needs to be performed in the intact nanoemulsions. With this in mind, we employed the method developed by Romsted and Bravo-Díaz [29,38,40], based on the application of the formalism of pseudophase kinetic model to the rapid reduction of the chemical probe 4- hexadecylbenzenediazonium ion, 16-ArN_2^+, by a phenolic antioxidant. The reaction occurs exclusively in the interfacial regions of the nanoemulsions [29,40]. The method allows separation of the medium (k_l) and concentration (P_O^l, P_W^l) contributions to the measured rate constant k_{obs}. Details of the procedure are given in the experimental section and in a number of literature reports [29, 40].

The obtained P_O^l, P_W^l and k_l values for the different antioxidants are reported in Table 1. k_l values for the C3-C12 derivatives are basically constant with an average value of $k_l = (31 \pm 3) \times 10^{-2}$ M^{-1} s^{-1}. Formally, k_l values are not strictly necessary to determine the partition constants P_O^l and P_W^l of the antioxidants, but provide useful information because they reflect potential changes in the location of the AOs and in the mechanisms of the reaction between the chemical probe and the AOs [29,38]. k_l values reflect the medium properties and thus constant k_l values suggest that the phenolic moieties of all AOs are located in a similar chemical environment (the interfacial region of the emulsion).

Table 1
Values for the partition constants P_O^l, P_W^l of gallic acid and alkyl gallates and for the rate constant k_l in the interfacial region of 1:9 olive O/W nanoemulsions. Values were determined in the intact nanoemulsions.

AO	10^2 k_l (M^{-1} s^{-1})	P_O^l	P_W^l
GA	12.3 ± 0.8	...	93 ± 11
C1	...	...	94 ± 7
C3	28 ± 3	161 ± 42	140 ± 22
C4	37 ± 9	86 ± 11	258 ± 41
C8	37 ± 1	28 ± 4	...
C12	28 ± 1	25 ± 5	...

The distribution of the AOs was determined by employing the partition constant P_W^I and P_O^I values in Table 1 using the equations indicated in the experimental section. Fig. 4 shows the variations of the percentage of antioxidants in the aqueous (%AO_W), oil (%AO_O) and interfacial (%AO_I) regions of the nanoemulsions.

Analyses of the data in Fig. 4 indicates that a significant fraction of the antioxidants (>30%) is found in the interfacial region (Fig. 4B) at Φ_I = 0.0047, increasing up to 70–90% when Φ_I = 0.037 depending on the hydrophobicity of the antioxidant). On the contrary, the fraction of antioxidant in the aqueous (Fig. 4A) and in the oil (Fig. 4C) regions decrease upon increasing Φ_I, so that at Φ_I = 0.0378, less than 30% of the AOs are located in the aqueous region and less than 15% in the oil region. Solid lines drawn to aid the eye.

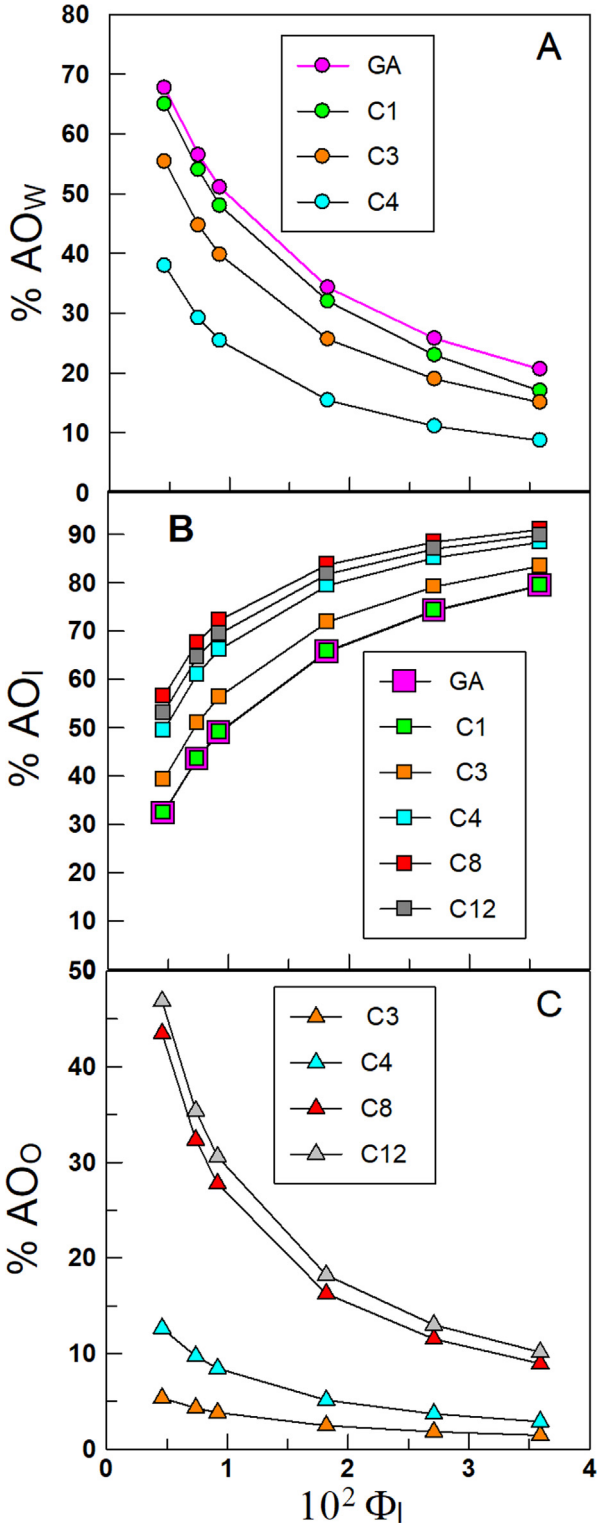

Fig. 4. Distribution of gallic acid derivatives in the various regions of 1:9 (v:v) olive nanoemulsions stabilized with Tween 80. W: aqueous, I: interfacial, O: oil. T = 25 °C.

Fig. 5 shows that the changes of both %(AO_I) and τ_{ind} with the hydrophobicity of the antioxidants parallel each other, contrary to those of τ_{ind} with %(AO_w) and %(AO_O) (plots not shown). These results demonstrate that there is a direct relationship between the oxidative stability of the nanoemulsions and the percentage of the antioxidant in the interfacial region but not with those in the aqueous and oil regions. This observation is important because it opens a new way to optimize the efficiency of antioxidants by modulating their hydrophobicity [31,44].

3.4. Relationships between the rate of the inhibition reaction and the effective antioxidant concentrations

The rate of the inhibited chemical reactions (5) in Scheme 1 depends on the local concentrations of the antioxidants at the reaction site. Thus, to make a proper interpretation of the oxidation kinetic results, determination of the interfacial concentrations of the AOs is required. Calculations are shown in the experimental section. For the sake of clarity in the ongoing discussion, the stoichiometric concentration, [AO_T], is expressed in moles per liter of total volume of emulsion, meanwhile effective concentrations in the various regions are indicated in parenthesis, (AO), and are given in moles per liter of the particular region. The volume of the interfacial region is equalt to the molar volume of the surfactant ($V_I = V_{surf}$).

Fig. 6 shows that, for any AO, the effective concentration in the aqueous and oil regions are similar to, or lower than, the stoichiometric concentration, $[AO_T] = 1 \times 10^{-4}$ M. The effective concentrations in the aqueous regions are ~10 times lower ($(AO_W) \approx 10^{-5}$ M) and decrease rapidly upon increasing both the hydrophobicity of the antioxidant and Φ_I. The effective concentration in the oil region, (AO_O), is similar to, or higher than (up to 10 fold) the stoichiometric concentration. As expected, (AO_O) increases upon increasing the hydrophobicity of the antioxidants but decreases upon increasing Φ_I.

It is, indeed, noticeable the much higher effective concentration of the AOs in the interfacial region, which can be up to 120 fold that

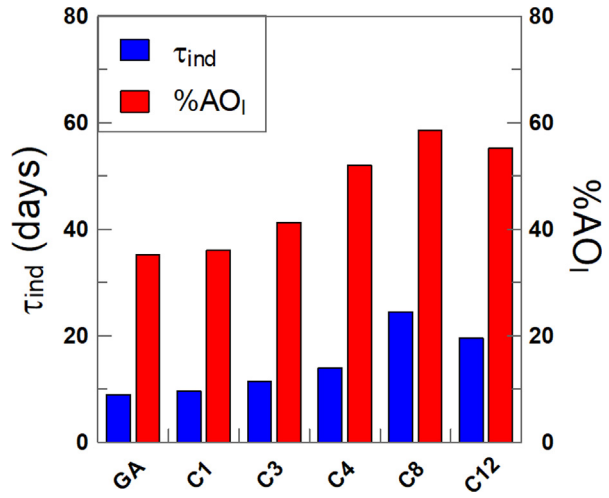

Fig. 5. Changes in %(AO_I) and τ_{ind} with the length of the alkyl chain of gallic acid derivatives (Φ_I = 0.005). Data extracted from Figs. 3B and 4B.

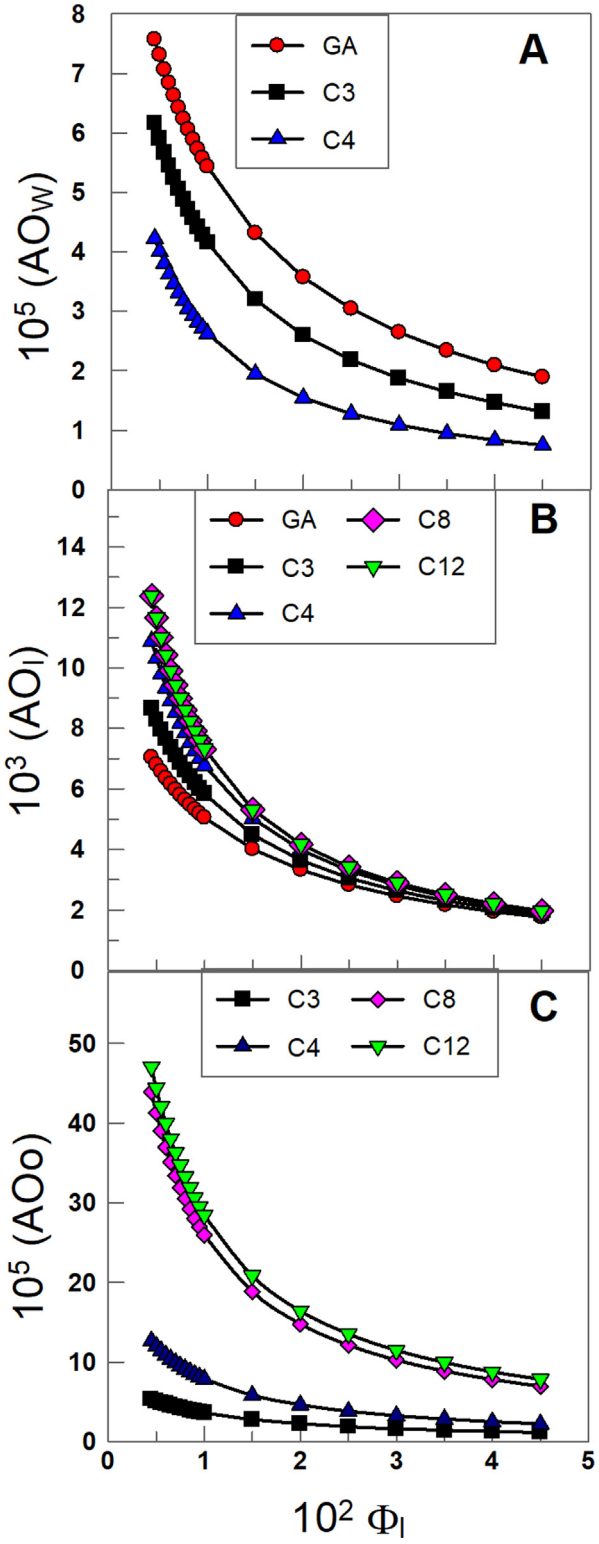

Fig. 6. Local concentrations (moles per liter of the region volume) of gallic acid derivatives and their variations with Φ_I in the aqueous (W), interfacial (I) and oil (O) regions [AO_T] = 0.1 mM. Solid lines drawn to aid the eye.

of the stoichiometric concentration. This means that AOs are accumulated in the interfacial region of the nanoemulsions and, thus, the rates of the inhibition reaction (reaction (5) in Scheme 1) should be much higher than those in bulk solution, making that the efficiency of antioxidants accumulated in the interfacial region to be much higher than that of those predominantly located in the oil or aqueous regions [29,38].

We note that an increase in Φ_I results in a dilution of the AOs in the interfacial region, as shown in Fig. 6B, so that for any AO, (AO_I) decreases asymptotically upon increasing Φ_I. The reason of this decrease is because, for any AO at fixed O/W ratio, the increase in the % AO_I does not compensate the increase in the interfacial volume (Eq. (9)) and a net dilution effect takes place [29,38].

To further corroborate the hypothesis, we compared the variations in the local concentrations of the antioxidants in the oil and in the interfacial regions with the alkyl chain with those of the induction times τ_{ind}, Fig. 7. As shown, plots for the variations of τ_{ind} and (AO_I) parallel each other but not those with (AO_O), providing strong (and quantitative) evidence supporting the idea that the main reaction site for the reaction between peroxyl radicals and AOs in a multiphasic systems is the interfacial region, as it was usually assumed in the past [10,45–47].

Results also show that the antioxidative interfaces of nanoemulsions (and, in general, of any colloidal system) can be boosted by increasing the operational interfacial concentrations of antioxidants. A comparison of τ_{ind} with the effective concentrations in the aqueous region is disregarded considering that the reaction between the antioxidants and peroxyl radicals is unlikely to take place in the aqueous region due to insolubility of lipids in water and also the effective antioxidant concentrations are much lower than the stoichiometric concentrations, Fig. 6C.

Thus, the full picture for the inhibition reaction can be depicted as in Scheme 5, which shows some basic properties of the domains of O/W nanoemulsions (and emulsions) and of the distribution of reactants. We can observe the following features: I) the typical values for the dielectric constants of each region, II) the time-average

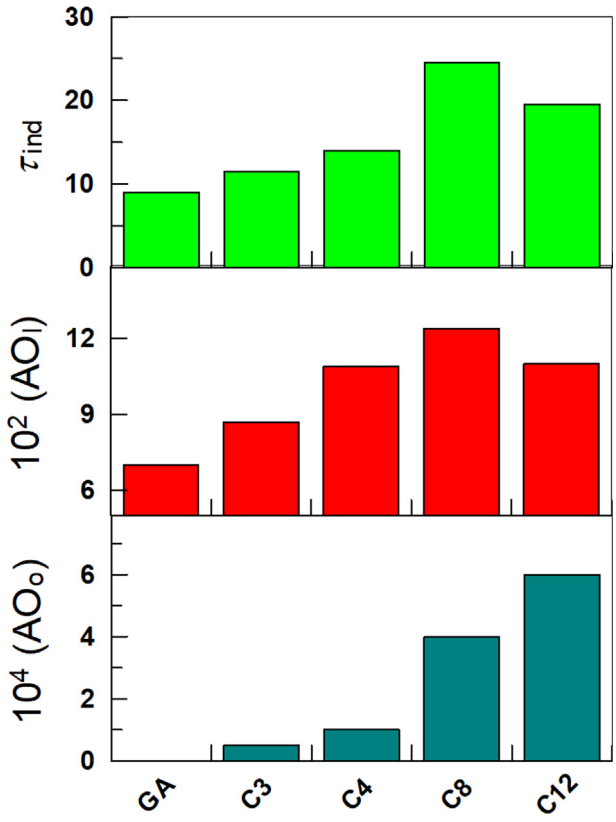

Fig. 7. Variations of τ_{ind} (days) and of the actual concentrations of AOs in the interfacial, and oil regions of olive oil-in-water nanoemulsions (Φ_I = 0.005). The effective concentrations are given in moles of antioxidant per liter of region volume.

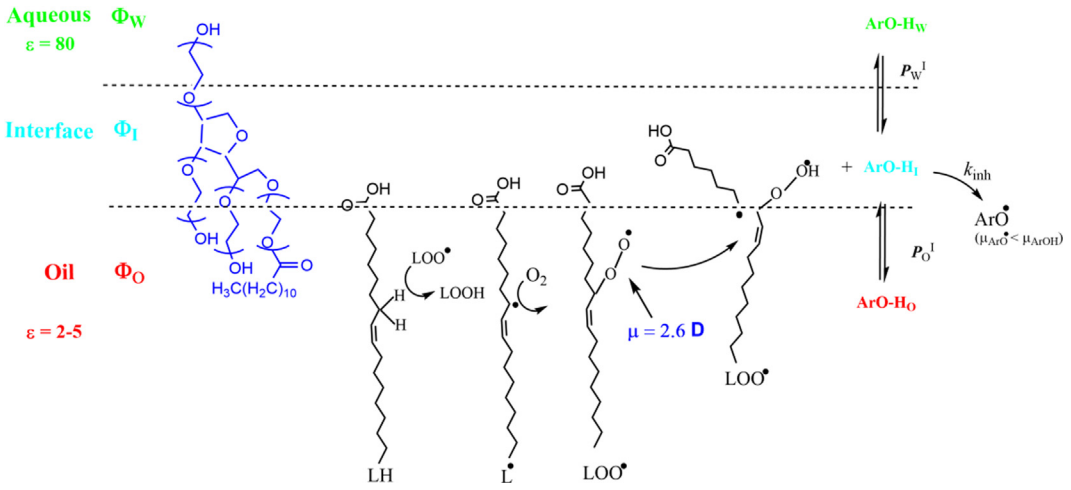

Scheme 5. Biophysical, three-region, model showing the various domains of an oil-in-water nanoemulsion droplets, the distribution of an antioxidant between the three regions and the fate of a fatty acid molecule undergoing oxidation before reacting with an antioxidant (reaction (5) in Scheme 1). Values for the dielectric constants of the oil and aqueous regions and of the dipole moment of the formed peroxyl radical are indicated to envisage the motion of the peroxyl radical towards the interfacial region. The positions and orientations of the molecules are time-averaged and are shown for illustrative purposes.

location of a partitioning ground-state antioxidant of moderate hydrophobicity, and III) the dipole moment of a PUFA molecule and that of the corresponding radical LOO·. Upon H-abstraction, the dipole moment for the antioxidant is lowered and promoting its diffusion into the droplets core.

Because fluid emulsions are in dynamic equilibrium [29,48], we can assume, in principle, that the reaction between the antioxidant and the peroxyl radical take place in any of the three regions of the nanoemulsions. Thus, the rate of the inhibition reaction will be given by the sum of the rates in each region, Eq. (10) [29,38].

$$r_{inh} = r_{inh(W)} + r_{inh(I)} + r_{inh(O)} = \\ = nk_{inh(W)}(LOO^{\cdot}_{W})(AO_W) + nk_{inh(I)}(LOO^{\cdot}_{I})(AO_I) + nk_{inh(O)}(LOO^{\cdot}_{O})(AO_O) \quad (10)$$

In Eq. (10), k stand for the rate constants and magnitudes in parenthesis, (), indicate the effective concentration of reactants in the aqueous (w), interfacial (I) and oil (O), expressed as moles per liter of a particular region and n is the so-called stoichiometric factor (number of peroxyl radicals trapped by a single antioxidant molecule) [21].

However, and as we mentioned above, significant reaction in the aqueous region is unlikely to occur because fatty acids are water insoluble and their concentration, i.e., [LOO·] ≈ 0) and therefore $r_{inh(W)}$ is negligible. The reaction may start in the bulk, PUFA-rich, oil core of the nanoemulsions droplet, but the dipole moment of the generated lipoperoxide radical LOO· is quite high (2.6 D) and tends to diffuse to the interfacial region of the droplet [21,49,50]. However, it is not likely that a significant fraction of the inhibition reaction takes place in the oil region because the variations of τ_{ind} with (%AO_O) diverge, Fig. 7. Thus, the main inhibition reaction is likely to take place at the interfacial region (as, otherwise, it was assumed for a long time) where the antioxidant reacts with LOO· yielding LOOH and an antioxidant radical $A_rO^{\cdot}$ [17–19,44].

Thus, Eq. (10) can be simplified and the rate of the inhibition reaction is given by Eq. (11), which predicts that the rate of inhibition depends, among others, on the interfacial antioxidant concentration as it was observed experimentally (Fig. 7).

$$r_{inh} \approx r_{inh(I)} = nk_{inh(I)}(LOO^{\cdot}_{I})(AO_I) \quad (11)$$

The importance of this interfacial region has been previously highlighted by different researchers and attempts are made to get as much information as possible on this highly anisotropic region [29,40,51]. However, some difficulties arise because of the physical impossibility of separating the interfacial region from the aqueous or oil ones without disrupting the existing equilibria, making that the determination of any physical parameter to characterize the region needs to be achieved in intact emulsions.

Indeed, most food and biochemical important peroxidation processes take place at the water-oil interfaces of colloidal systems, which can be considered, in a first approach, as multiphasic systems composed of three regions with different solvent properties.

Literature reports on the kinetics and mechanism of these reactions in micellar systems demonstrate that the kinetics of peroxidation follow the same rate laws as for homogeneous solutions, but require considering the corresponding rate constants at the various reaction sites and the partitioning of reactants between regions, and therefore a thorough description of the oxidation reaction requires to take into account the partitioning of the reactants between the various domains of the colloidal system as shown in Scheme 4 [21,29,40,49].

Taken together, partitioning and oxidation results show that the main parameter that controls the efficiency of the AOs in nanoemulsions is their effective concentration in the interfacial region, which depends on the hydrophobicity of the antioxidant and the emulsifier concentration employed in the preparation of the nanoemulsions. The results show a practical approach to boost the antioxidant effectiveness in interfaces of nanoemulsions by employing potent and natural antioxidant by attaching inert alkyl chain of variable length to optimize its hydrophobicity. For instance, the interfacial molarity of the C8 derivative is 120 times higher than its stoichiometric concentration when Φ_I = 0.005, decreasing ~6 fold upon increasing Φ_I to 0.04, Fig. 6, and that a further increase in the hydrophobicity is not compensated by an increase in the interfacial concentration, on the contrary, it decreases slightly because the increase in hydrophobicity makes C12 to be transferred to the oil region.

4. Rates of initiation of olive oil oxidation in nanoemulsions

In all oxidation experiments carried out in this work, no radical initiator like AAPH or ionizing radiation was employed, and all samples were simultaneously allowed to spontaneously oxidize in the dark to minimize the deleterious effects of light and (see experimental section). So, we can safely assume that the main ini-

Table 2
Values of the length of the induction periods (obtained from the oxidation reactions shown in Fig. 3A), the effective interfacial concentrations (extracted from Fig. 6) and of the ratio r_i/n (Eq. (3)). * moles of antioxidant per liter of interfacial volume.

	Control	GA	C1	C3	C4	C8	C12
τ_{ind} (days)	6	10	10	12	15	22	17
10^3 (AO_l) (M)*	–	6.8	6.8	8.3	10.3	11.6	10.9
10^4 r_i/n (M $days^{-1}$)		6.8	6.8	6.9	6.9	5.3	6.4

tiation pathway is the thermal decomposition of the lipid, most probably through the reaction with oxygen (2LH + O_2 → 2L· + H_2O_2), a reaction that has an activation energy much lower than the direct thermal cracking process [52,53].

In the absence of antioxidants, reaction (3) (Scheme 1) is the rate-limiting step, but in the presence of antioxidants, reaction (5) (Scheme 1) becomes the main reaction pathway and lipid radicals may be terminated by the rate-limiting process shown in reaction (5) is rate-determining and the rate constant k_{inh} is the rate constant that describes the efficiency of the antioxidant when compared to k_p (reaction (3)). Reaction (6) describes the fate of radicals derived from the antioxidant, establishing the number **n** of radicals trapped by each antioxidant. This parameter is usually known as the stoichiometric factor, and its value is generally close to n = 2 for most phenolic antioxidants [14,20,21,50,52].

Thus, assuming that in the presence of antioxidants reactions (5) and (6) are the major routes for LOO· annihilation, Eq. (12) can be derived by applying the steady-state condition to all radical species and by assuming that LH and O_2 consumption are not limiting (i.e., their concentrations remain essentially constant) [14,20,32].

$$r_i = \frac{n(\text{Ar - OH}_l)}{\tau_{ind}} \tag{12}$$

It is worth noting that Eq. (12) was first derived for reactions taking place in bulk solution [21,49,54], where reactants are not partitioned and, in the literature, it is commonly expressed in terms of the corresponding antioxidant stoichiometric concentration [Ar-OH_T]. However, the oxidation reactions in nanoemulsions requires to take into consideration the antioxidant partitioning and, therefore, the effective antioxidant concentration at the reaction site should be employed in Eq. (12), which according to results in Fig. 7, is the interfacial region.

For an homologous series of antioxidants having the same reactive moiety, the value of *n* in Eqs. (10)–(12) (3) (number of radicals trapped by the antioxidant) should be very similar if not the same [21,49,52], and thus we can assume that the rate of initiation r_i only depends on the ratio between the "effective" concentration of the antioxidants in the interfacial region, (AO_l), and the length of the inhibition period τ_{inh}. Because the oil is the same in all experiments and was oxidized under the same thermal conditions, the rate of initiation, or more precisely, the ratio r_i/n should be independent of the antioxidant employed. Table 2 shows the calculated values for r_i/n being basically the same for GA and the C1-C4 derivatives, but slightly lower for the C8 and C12 ones.

The low r_i/n values found for the C12 and for the C8 derivatives can be, tentatively, explained bearing in mind that the alkyl chain of these antioxidants provide a critical hydrophobicity (so called "cut-off" effect) sensitive to slight fluctuations in their interfacial concentrations due to changes, for instance, in the orientation of the reactive moiety in the interface region [55,56] or slight changes in the stoichiometric (n) value [21]. In fact, the constancy in the r_i/n values for the C1-C4 suggests that, under our experimental conditions, the rate of production of radicals is rather constant in spite that we did not used an initiator as is commonly done in quantitative oxidation experiments, and we cannot rule out some fluctuations in spite that the experimental conditions employed do not seem to affect seriously the rates of initiation. Literature reports indicate that the reactivity of antioxidants grafter with alkyl chains do not have a significant effect on their reactivity on various radicals, and thus an effect of alkylation on the antioxidant efficiency is discarded [19,23,44,47,57,58].

Another possible explanation may be related to the fact that the distribution experiments were carried out at T = 25 °C, meanwhile the oxidation ones were carried out at T = 60 °C. This means that, reasonably, one could argue that the effective interfacial concentrations may not be the same at T = 25 °C and T = 60 °C. This hypothesis seems unlikely at least for GA, because we previously investigated the effects of temperature on the distribution of GA, and demonstrated that changes in T have only a modest effect on the distribution of GA and do not modify significantly its interfacial concentrations [39]. The constancy in the r_i/n values for the C1-C4 suggests that changes in T do not have a major effect on the distributions of these antioxidants.

However, when analyzing the effects of T on the distribution of hydrophobic antioxidants such as α-tocopherol [59], we found a slight dependence of the distribution of TOC between the oil and interfacial regions, and thus a change in T may affect the effective interfacial concentration of C12 and mainly the C8 derivatives [44,60]. The dependence of interfacial concentrations with T, as well as other hypothesis, are currently being explored and will be part of future reports.

5. Conclusions

Lipid oxidation is still a major challenge to minimize food spoilage and waste and to improve the sustainability of the food supply. Much of the early kinetic research focused on chemical mechanisms of lipid oxidation in bulk solution, but real foods are multiphasic systems, and require a deeper knowledge on how the solvent properties of the various domains and the distribution of reactants affect the oxidation kinetics and its inhibition by antioxidants [22,45,46,51]. In addition, research in oil-in-water emulsions is particularly important because most oils are not consumed in their bulk form but are instead dispersed into foods as colloidal droplets.

According to Decker et al. [61], the pseudophase method employed here constitute a large improvement over other methods in that direct measurement of antioxidants associated with surfactants can be made. We believe that the kinetic methodology presented herein is robust, trustable, and can complement methods aimed at studying lipid peroxidation [62–64]. Other researchers [65] suggested that to demonstrate the real power and utility of pseudophase kinetic models, direct correlations between antioxidant efficiencies and different properties in interfaces (such as the effective interfacial concentration) should be achieved and proved. Here, we confirmed that, in the absence of artificial initiators (which helps to eliminate complications derived from potential interactions between antioxidants and the initiator), the ratio of the effective interfacial concentrations and the length of the induction periods is constant and independent of the hydrophobicity of the antioxidant employed. This certainly provides a strong support to the use of pseudophase methods to determine interfa-

cial concentrations [29,38,40] and also supports the direct relationship between antioxidant efficiencies and effective interfacial concentrations, suggesting, at the same time, that additional hypothesis suggested by other researchers, such as if micelles or reverse micelles affect the distribution of antioxidants or if the size and shape of droplets in emulsions affect antioxidant distribution [61,66], to be less reliable.

The work is far from being finished because important problems such as the prediction of the best antioxidant or set of antioxidants to minimize the oxidation of foods is far from being completely understood, and further investigations regarding the use of different oils, new compounds with potential antioxidant activity, or even the identification of mixtures of antioxidants which may lead to synergetic or antagonist effects are required [67], together with the development of new procedures for determining antioxidant and radical distributions [55,56,68] as well as determining the kinetics and mechanisms of the reactions involved [32,63]. Future work will be aimed at comparing different antioxidants and finding a quantitative measure of the initiation rate in the absence of artificial initiators. The results can be useful for the food and pharmaceutical industry to deal with the inherent rancidity problem of highly unsaturated natural oils such as those containing valuable omega-3 fatty acids.

CRediT authorship contribution statement

Marlene Costa: Data curation, Writing - review & editing. **Josefa Freiría:** Data curation, Writing - review & editing. **Sonia Losada:** Conceptualization, Methodology, Data curation, Writing - review & editing. **Fátima Paiva-Martins:** Methodology, Writing - review & editing. **Carolina Aliaga:** Writing - review & editing. **Carlos Bravo-Díaz:** Conceptualization, Methodology, Writing - original draft, Writing - review & editing.

Declaration of Competing Interest

The authors declare that they have no known competing financial interests or personal relationships that could have appeared to influence the work reported in this paper.

Acknowledgement

This manuscript was prepared during a sabbatical leave of C. B-D, supported by Universidad de Vigo. Financial support of the following institutions acknowledged: Red de Uso Sostenible de los Recursos Naturales y Agroalimentarios (REDUSO, Xunta de Galicia, Grant number ED431D 2017/18), FEDER (COMPETE), FCT – Fundação para a Ciência e a Tecnologia (UID/QUI/50006/2013 – POCI-01-0145-FEDER-007265), and Universities of Vigo and Porto. MC thanks FCT for the doctoral grant 509 (SFRH/BD/100889/2014). S. L-B thanks University of Vigo (Talent Recruitment Program 2018). C. A. thanks to 1160486, 1200192 FONDECYTANID-Chile and CEDENNA AFB180001 projects.

References

[1] C.C. Akoh, D.B. Min, Food Lipids: Chemistry, Nutrition, And Biotechnology, 2008.
[2] W. Manzanares, P. Langlois, G. Hardy, Intravenous lipid emulsions in the critically ill: an update, Curr. Opin. Crit. Care 22 (2016) 308–315.
[3] E. Muro, G.E. Atilla-Gokcumen, U.S. Eggert, Lipids in cell biology: how can we understand them better?, Mol. Biol. Cell 25 (2014) 1819–1823.
[4] A.R. Thiam, R.V. Farese Jr, T.C. Walther, The biophysics and cell biology of lipid droplets, Nat. Rev. Mol. Cell Biol. 14 (2013) 775–786.
[5] P.C. Calder, Lipids for intravenous nutrition in hospitalised adult patients: a multiple choice of options, Proc. Nutr. Soc. 72 (2013) 263–276.
[6] R. Mozuraityte, V. Kristinova, T. Rustad, in: Encyclopedia of Food and Health, Academic Press, Oxford, 2016, pp. 186–190, https://doi.org/10.1016/B978-0-12-384947-2.00508-0.
[7] E. Birben, U.M. Sahiner, C. Sackesen, S. Erzurum, O. Kalayci, Oxidative stress and antioxidant defense, World Allergy Organ. J. 5 (2012) 9.
[8] K.M. Schaich, F. Shahidi, Y. Zhong, N.A.M. Eskin, Biochemistry of Foods, third ed., Academic Press, San Diego, 2013, pp. 419–478. 10.1016/B978-0-08-091809-9.00011-X.
[9] K.M. Schaich, in: F. Shahidi (Ed.), Bailey's Industrial Oil and Fat Products, vol. 6, J. Wiley & Sons, NY, 2005, pp. 269–355.
[10] E.N. Frankel, Lipid Oxidation, The Oily Press, PJ Barnes & Associates, Bridgwater, England, 2005.
[11] F. Shahidi, P. Ambigaipalan, Phenolics and polyphenolics in foods, beverages and spices: antioxidant activity and health effects – a review, J. Funct. Foods 18 (Part B) (2015) 820–897.
[12] F. Shahidi, Handbook of Antioxidants for Food Preservation, first ed., Woodhead Pub, 2015.
[13] F.M.F. Roleira, E.J. Tavares-da-Silva, C.L. Varela, S.C. Costa, T. Silva, J. Garrido, F. Borges, Plant derived and dietary phenolic antioxidants: Anticancer properties, Food Chem. 183 (2015) 235–258.
[14] G. Litwinienko, A. Kamal-Eldin, J. Pokorny, Analysis of Lipid Oxidation, 2005.
[15] K.U. Ingold, D.A. Pratt, Advances in radical-trapping antioxidant chemistry in the 21st century: a kinetics and mechanisms perspective, Chem. Rev. 114 (2014) 9022–9046.
[16] L. Valgimigli, D.A. Pratt, Encyclopedia of Radicals in Chemistry, Biology and Materials, 2012.
[17] J. Freiría-Gándara, S. Losada-Barreiro, F. Paiva-Martins, C. Bravo-Díaz, Enhancement of the antioxidant efficiency of gallic acid derivatives in intact fish oil-in-water emulsions through optimization of their interfacial concentrations, Food Funct. 9 (2018) 4429–4442.
[18] I. Ferreira, M. Costa, S. Losada-Barreiro, F. Paiva-Martins, C. Bravo-Díaz, Modulating the interfacial concentration of gallates to improve the oxidative stability of fish oil-in-water emulsions, Food Res. Int. 112 (2018) 192–198.
[19] O. Mitrus, M. Żuraw, S. Losada-Barreiro, C. Bravo-Díaz, F. Paiva-Martins, Targeting antioxidants to interfaces: control of the oxidative stability of lipid-based emulsions, J. Agric. Food Chem. 67 (2019) 3266–3274.
[20] I. Pinchuk, H. Shoval, Y. Dotan, D. Lichtenberg, Evaluation of antioxidants: scope, limitations and relevance of assays, Chem. Phys. Lipids 165 (2012) 638–647.
[21] L. Ross, C. Barclay, M.R. Vinqvist, in: Z. Rappoport (Ed.), The Chemistry of Phenols, J. Wiley & West Sussex, England, 2003 (ch. 12).
[22] T. Waraho, D.J. McClements, E.A. Decker, Mechanisms of lipid oxidation in food dispersions, Tr. Food Sci. Technol. 22 (2011) 3–13.
[23] M. Costa, J. Freiría-Gándara, S. Losada-Barreiro, F. Paiva-Martins, C. Bravo-Díaz, Effects of droplet size on the interfacial concentrations of antioxidants in fish and olive oil-in-water emulsions and nanoemulsions and on their oxidative stability, J. Colloid Interface Sci. 562 (2020) 352–362.
[24] S. Losada-Barreiro, C. Bravo-Díaz, Free radicals and polyphenols: the redox chemistry of neurodegenerative diseases, Eur. J. Med. Chem 133 (2017) 379–402.
[25] D. Turck, J.-L. Bresson, B. Burlingame, T. Dean, S. Fairweather-Tait, M. Heinonen, K.I. Hirsch-Ernst, I. Mangelsdorf, H.J. McArdle, A. Naska, M. Neuh€auser-Berthold, G. Nowicka, K. Pentieva, Y. Sanz, A. Sj€odin, M. Stern, T.D.H. Van Loveren, M. Vinceti, P. Willatts, A. Martin, J.J. Strain, L. Heng, S. Valtuena-Martínez, A. Siani, Guidance for the scientific requirements for health claims related to antioxidants, oxidative damage and cardiovascular health, EFSA 16 (2018) 5136–5137.
[26] EFSA, in EFSA Panel on Food additives and Nutrient Sources added to Food, EFSA J. 13(10) (2015) 4248 (2015, vol. 12, pp. 3642-3646).
[27] M. Rose, Scientific Opinion on the re-evaluation of propyl gallate (E 310) as a food additive EFSA Panel on Food additives and Nutrient Sources added to Food (ANS), 2014.
[28] M. Laguerre, L.J. López-Giraldo, J. Lecomte, M.J. Figueroa-Espinoza, B. Baréa, J. Weiss, E.A. Decker, P. Villeneuve, Chain length affects antioxidant properties of chlorogenate esters in emulsion: the cut-off theory behind the polar paradox, J. Agric. Food Chem 57 (2009) 11335–11342.
[29] C. Bravo-Díaz, L.S. Romsted, C. Liu, S. Losada-Barreiro, M.J. Pastoriza-Gallego, X. Gao, Q. Gu, G. Krishnan, V. Sánchez-Paz, Y. Zhang, A. Ahmad-Dar, To model chemical reactivity in heterogeneous emulsions, think homogeneous microemulsions, Langmuir 31 (2015) 8961–8979.
[30] M. Costa, S. Losada-Barreiro, F. Paiva-Martins, C. Bravo-Diaz, Optimizing the efficiency of antioxidants in emulsions by lipophilization: tuning interfacial concentrations, RSC Adv. 6 (2016) 91483–91493.
[31] M. Meireles, S. Losada-Barreiro, M. Costa, F. Paiva-Martins, C. Bravo-Díaz, L. S. Monteiro, Control of antioxidant efficiency of chlorogenates in emulsions: modulation of antioxidant interfacial concentrations, J. Sci. Food Agric. (2020).
[32] Z. Zielinski, N. Presseau, R. Amorati, L. Valgimigli, D.A. Pratt, J. Am. Chem. Soc. 136 (2014) 1570.
[33] J.W. Spray, Review of intravenous lipid emulsion therapy, J. Infusion Nursing: Off. Publ. Infusion Nurses Soc. 39 (2016) 377–380.
[34] G.L. Fell, P. Nandivada, K.M. Gura, M. Puder, Intravenous lipid emulsions in parenteral nutrition, Adv. Nutr. 6 (2015) 600–610.
[35] P.C. Calder, G.L. Jensen, B.V. Koletzko, P. Singer, G.J.A. Wanten, Lipid emulsions in parenteral nutrition of intensive care patients: current thinking and future directions, Intensive Care Med. 36 (2010) 735–749.

[36] S. Losada-Barreiro, C. Bravo Díaz, F. Paiva Martins, L.S. Romsted, Maxima in antioxidant distributions and efficiencies with increasing hydrophobicity of gallic acid and its alkyl esters. The pseudophase model interpretation of the Cut-off effect, J. Agric. Food Chem 61 (2013) 6533–6543.
[37] P. Lisete-Torres, S. Losada-Barreiro, H. Albuquerque, V. Sánchez-Paz, F. Paiva-Martins, C. Bravo-Díaz, Distribution of hydroxytyrosol and hydroxytyrosol acetate in olive oil emulsions and their antioxidant efficiency, J. Agric. Food Chem. 60 (2012) 7318–7325.
[38] L.S. Romsted, C. Bravo-Díaz, Modelling chemical reactivity in emulsions, Curr. Opin. Colloid Interface Sci. 18 (2013) 3–14.
[39] S. Losada-Barreiro, V. Sánchez Paz, C. Bravo Díaz, F. Paiva Martins, L.S. Romsted, Temperature and emulsifier concentration effects on gallic acid distribution in a model food emulsion, J. Colloid Interface Sci. 370 (2012) 73–79.
[40] A.A. Dar, C. Bravo-Diaz, N. Nazir, L.S. Romsted, Chemical kinetic and chemical trapping methods: unique approaches for determining respectively the antioxidant distributions and interfacial molarities of water, counter-anions, and other weakly basic nucleophiles in association colloids, Curr. Opin. Colloid Interface Sci. 32 (2017) 84–93.
[41] M. Costa, S. Losada-Barreiro, F. Paiva-Martins, C. Bravo-Díaz, Physical evidence that the variations in the efficiency of homologous series of antioxidants in emulsions are a result of differences in their distribution, J. Sci. Food Agric. 97 (2017) 564–571.
[42] M. Costa, S. Losada-Barreiro, F. Paiva-Martins, C. Bravo-Díaz, L.S. Romsted, A direct correlation between the antioxidant efficiencies of caffeic acid and its alkyl esters and their concentrations in the interfacial region of olive oil emulsions. The pseudophase model interpretation of the "cut-off" effect, Food Chem 175 (2015) 233–242.
[43] P. Balgavý, F. Devínsky, Cut-off effects in biological activities of surfactants, Adv. Colloid. Interf. Sci. 66 (1996) 23–63.
[44] E.A. Raimúndez-Rodríguez, S. Losada-Barreiro, C. Bravo-Díaz, Enhancing the fraction of antioxidants at the interfaces of oil-in-water emulsions: a kinetic and thermodynamic analysis of their partitioning, J. Colloid Interface Sci. 555 (2019) 224–233.
[45] C.C. Berton-Carabin, M.-H. Ropers, C. Genot, Lipid oxidation in oil-in-water emulsions: involvement of the interfacial layer, Compr. Rev. Food Sci. Food Safety 13 (2014) 945–977.
[46] C. Berton, M.H. Ropers, M. Viau, C. Genot, Contribution of the interfacial layer to the protection of emulsified lipids against oxidation, J. Agric. Food Chem. 59 (2011) 5052–5061.
[47] D. Kahveci, M. Laguerre, P. Villeneuve, in: Polar Lipids, Elsevier, 2015, pp. 185–214. https://doi.org/10.1016/B978-1-63067-044-3.50011-X.
[48] C. Bravo-Díaz, L.S. Romsted, S. Losada-Barreiro, F. Paiva-Martins, Using a pseudophase model to determine AO distributions in emulsions: why dynamic equilibrium matters, Eur. J. Lipid Sci. Technol. 119 (2017) 1600277.
[49] A.R. Waldeck, R. Stocker, Radical-initiated lipid peroxidation in low density lipoproteins: insights obtained from kinetic modeling, Chem. Res. Toxicol. 9 (1996) 954–964.
[50] J. Jodko-Piórecka, J. Cedrowski, G. Litwinienko, in: R. Apak, E. Capanoglu, F. Shahidi (Eds.), Measurement of Antioxidant Activity & Capacity: Recent Trends and Applications, J. Wiley & Sons, 2018, pp. 225–272. https://doi.org/10.1002/9781119135388.ch12.
[51] C.C. Berton-Carabin, L. Sagis, K. Schroën, Formation, structure, and functionality of interfacial layers in food emulsions, Annu. Rev. Food Sci. Technol. 9 (2018) 551–587.
[52] K.U. Ingold, Inhibition of the autoxidation of organic substances in the liquid phase, Chem. Rev. 61 (1961) 563–589.
[53] E.T. Denisov, I.B. Afanasév, Oxidation and Antioxidants in Organic Chemistry and Biology, CRC Press, Boca Raton, FL, USA, 2005.
[54] J.P. Cosgrove, D.F. Church, W.A. Pryor, The kinetics of the autoxidation of polyunsaturated fatty acids, Lipids 22 (1987) 299–304.
[55] C. Aliaga, F. Bravo-Moraga, G.D.S. Márquez, S. Lürh, G. Mena, M.C. Rezende, Location of TEMPO derivatives in micelles: subtle effect of the probe orientation, Food Chem. 192 (2016) 395–401.
[56] A. Lopez de Arbina, S. Losada-Barreiro, M.C. Rezende, M. Vidal, C. Aliaga, The location of amphiphobic antioxidants in micellar systems: The diving-swan analogy, Food Chem. 279 (2019) 288–293.
[57] M. Costa, S. Losada-Barreiro, C. Bravo-Díaz, A.A. Vicente, L.S. Monteiro, F. Paiva-Martins, Influence of AO chain length, droplet size and oil to water ratio on the distribution and on the activity of gallates in fish oil-in-water emulsified systems: emulsion and nanoemulsion comparison, Food Chem. 310 (2020) 125716.
[58] M. Laguerre, C. Bayrasy, J. Lecomte, B. Chabi, E.A. Decker, C. Wrutniak-Cabello, G. Cabello, P. Villeneuve, How to boost antioxidants by lipophilization?, Biochimie 95 (2012) 1–7.
[59] M.J. Pastoriza-Gallego, V. Sánchez-Paz, S. Losada-Barreiro, C. Bravo-Diaz, K. Gunaseelan, L.S. Romsted, Effects of temperature and emulsifier concentration on α-tocopherol distribution in a stirred, fluid, emulsion. Thermodynamics of α-tocopherol transfer between the oil and interfacial regions, Langmuir 25 (2009) 2646–2653.
[60] S. Losada-Barreiro, V. Sánchez-Paz, C. Bravo-Díaz, Transfer of antioxidants at the interfaces of model food emulsions: distributions and thermodynamic parameters, Org. Biomol. Chem. 6 (2008) 4004–4011 (2015, 13, 876-885).
[61] E.A. Decker, D.J. McClements, C. Bourlieu-Lacanal, E. Durand, M.C. Figueroa-Espinoza, J. Lecomte, P. Villeneuve, Hurdles in predicting antioxidant efficacy in oil-in-water emulsions, Tr. Food Sci. Technol. 67 (2017) 183–194.
[62] R. Félix, P. Valentão, P.B. Andrade, C. Félix, S.C. Novais, M.F.L. Lemos, Evaluating the in vitro potential of natural extracts to protect lipids from oxidative damage, Antioxidants 9 (2020) 231.
[63] F. Mollica, M. Lucarini, C. Passerini, C. Carati, S. Pavoni, L. Bonoldi, R. Amorati, Effect of antioxidants on high-temperature stability of renewable bio-oils revealed by an innovative method for the determination of kinetic parameters of oxidative reactions, Antioxidants 9 (2020) 399.
[64] A. Konopko, J. Kusio, G. Litwinienko, Antioxidant activity of metal nanoparticles coated with tocopherol-like residues-the importance of studies in homo- and heterogeneous systems, Antioxidants 9 (2020) 5.
[65] C. Genot, Distributions of phenolic acid antioxidants between the interfacial and aqueous regions of corn oil emulsions–a commentary, Eur. J. Lipid Sci. Technol. 117 (2015) 1684–1686.
[66] M. Laguerre, A. Bily, M. Roller, S. Birtić, Mass transport phenomena in lipid oxidation and antioxidation, Annu. Rev. Food Sci. Technol. 8 (2017) 391–411.
[67] V. Kancheva, S. Angelova, in: A. Catalá (Ed.), Lipid Peroxidation: Inhibition, Effects and Mechanisms, Nova Science Pub., 2017.
[68] C. Aliaga, F. Celis, S. Lürh, R. Oñate, TEMPO-attached pre-fluorescent probes based on pyridinium fluorophores, J. Fluorescence 25 (2015) 979–983.